Bulletin of the Seismological Society of America, Vol. 82, No. 4, pp. 1956–1963, August 1992

SHORT NOTES

FITTING THE STOCHASTIC ω^{-2} SOURCE MODEL TO OBSERVED RESPONSE SPECTRA IN WESTERN NORTH AMERICA: TRADE-OFFS BETWEEN $\Delta\sigma$ AND κ

BY DAVID M. BOORE, WILLIAM B. JOYNER, AND LEIF WENNERBERG

INTRODUCTION

The stochastic model of Hanks and McGuire (1981) has had impressive success in predicting earthquake ground motions over a broad range of magnitudes at near-source (e.g., Hanks and McGuire, 1981; Boore, 1983), regional (e.g., Hanks and Boore, 1984; Boore and Atkinson, 1987), and teleseismic distances (e.g., Boore, 1986). It is being used widely to produce ground motions for engineering design and seismological research (e.g., Atkinson, 1984; Boore and Atkinson, 1987; Toro and McGuire, 1987; Ou and Herrmann, 1990; Silva *et al.*, 1990; Chin and Aki, 1991; Rovelli *et al.*, 1991; Stepp *et al.*, 1991).

In its usual form, the model requires two main parameters, other than the basic description of source size (usually given by seismic moment): one to control acceleration spectral levels above the corner frequency and the other to specify the decay of the spectra at high frequencies. These two parameters are usually denoted by $\Delta\sigma$ (the stress parameter) and κ (the attenuation parameter of Anderson and Hough, 1984; the parameter f_{max} of Hanks, 1982, serves the same function).

In our applications of the stochastic model, we have chosen $\Delta\sigma$ and κ (or f_{max}) based on the studies of Hanks and McGuire and Anderson and Hough, and we found that the ground motions produced using these values are in reasonable agreement with observed motions (e.g., Boore, 1983; Joyner, 1984; Boore, 1986). We made no effort to derive $\Delta\sigma$ and κ from observed ground motions. We do that in this note, using the empirically derived equations of Joyner and Boore (1988) as a convenient description of observed ground motions.

METHODOLOGY

We subtracted the logarithms of the response-spectral ordinates found in the empirical analysis of Joyner and Boore (1988, Table 2) from the logarithms of the stochastic-model calculations to form residuals. We computed residuals for **M** = 5.5, 6.5, and, 7.5 at 10 of the 12 periods considered by Joyner and Boore (0.1, 0.15, 0.2, 0.3, 0.4, 0.5, 0.75, 1.0, and 2.0 sec; their periods of 3.0 and 4.0 sec were excluded because the quality of the empirical fits are questionable for those periods). A distance of 20 km was used. This distance is the horizontal distance r_0 in the Joyner and Boore equations. Joyner and Boore used a point source model as the basis for their regression equations and determined period-dependent pseudo-depths h that gave slant distances $r = \sqrt{r_0^2 + h^2}$. The stochastic model is also a point source model, and for consistency the slant distances used in the calculations were the same as used in the evaluation of the Joyner and Boore equations (in other words, r_0 was fixed at 20 km, but r depended on oscillator period, ranging from 20.54 km for T = 2.0 sec to 22.97 km for T = 0.1 sec).

Using the stochastic model, we evaluated the response spectra for 189 pairs of $\Delta\sigma$ and κ. The parameters were equally spaced in κ from $\kappa = 0.0$ to $\kappa = 0.10$ sec, and equally spaced in log $\Delta\sigma$ from $\Delta\sigma = 25$ to $\Delta\sigma = 400$ bars. A site amplification was used; this and other parameters are given in Tables 2 and 3 in Boore (1986). We used a smoothed variation (as given in Boore and Joyner, 1991) of the Joyner (1984) spectral shape with constant stress scaling, a ratio of the two corner frequencies of 4, and a critical magnitude of 7.0. Our conclusions remain unchanged if 7.5 is chosen for the critical magnitude. Random vibration theory (e.g., Joyner and Boore, 1988) was used for the calculations; spot checks using time-domain simulations were within 0.05 log units of the random vibration results, even for the response of the longest period oscillator ($T = 2.0$ sec) driven by the smallest earthquake ($\mathbf{M} = 5.5$).

Results

The residuals for $\mathbf{M} = 6.5$ and $r_0 = 20$ km are shown in Figure 1 for oscillator periods of 0.1 and 2.0 sec (a distance of 20 km and a magnitude of 6.5 is approximately in the middle of the magnitude-log distance distribution for the strong motion data set.) The contour plots look qualitatively as expected. There is slight dependence of the residuals on κ and $\Delta\sigma$ for long-period oscillators, but as the period decreases, the sensitivity to the parameters increases. The trade-off curve (the line of zero residual, for which the stochastic model exactly fits the empirical values) steepens as period is decreased.

The straight contour lines in Figure 1 indicate an exponential dependence of $\Delta\sigma$ on κ. This dependence is explained in the following by assuming that the computed response spectral values are proportional to the corresponding Fourier spectral amplitudes of the stochastic model at the period of the oscillator. Above

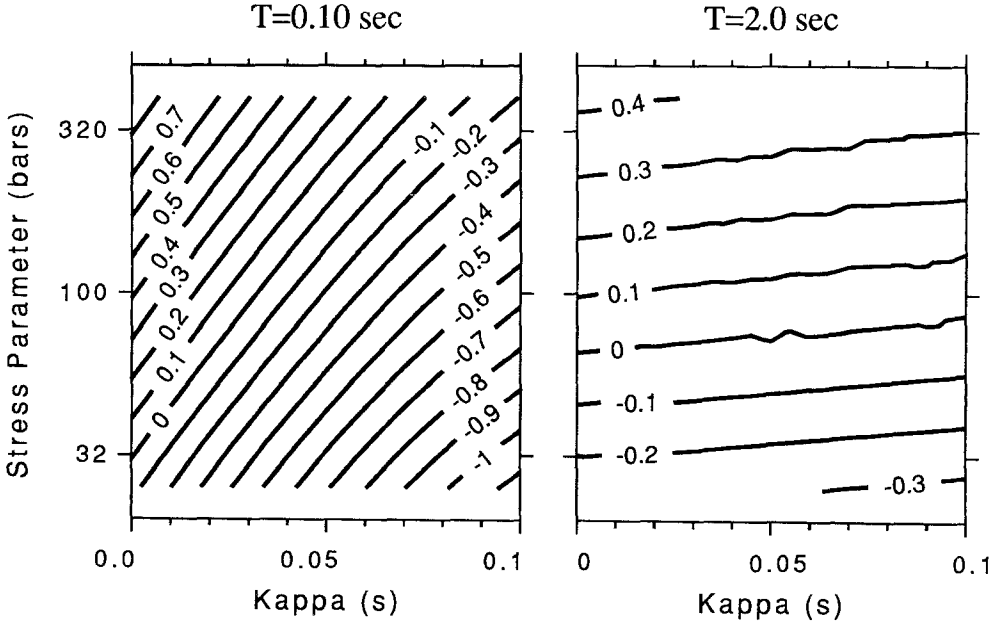

FIG. 1. Contours of residuals (predicted minus observed) for two oscillator periods, for $\mathbf{M} = 6.5$ and $r_0 = 20$ km.

the source corner frequency the trade-off curves are determined by the requirement that the spectral level be the same for values of κ and $\Delta\sigma$ on those curves. For the ω^{-2} source model this gives

$$M_0 f_c^2 e^{-\pi\kappa/T} = C(T), \tag{1}$$

where f_c is the corner frequency, and C depends only on T and on period-independent factors such as distance, seismic velocity, and density that determine the overall spectral level. From the scaling relation between corner frequency and stress parameter, we obtain

$$\Delta\sigma = D(T)\frac{e^{3\pi\kappa/2T}}{\sqrt{M_0}}, \tag{2}$$

where $D(T)$ is a period-dependent constant. Thus, for a constant spectral level there is an exponential dependence of $\Delta\sigma$ on κ and the slopes of the trade-off lines on a semilog plot increase for decreasing periods.

The ambiguity in the model parameters $\Delta\sigma$ and κ can be removed by plotting the trade-off curves for several periods; if the model were perfectly consistent with the data, the curves would intersect at a single value of κ and $\Delta\sigma$ (and this point of intersection would be the same for all magnitudes). We show in Figure 2a the trade-off curves for **M** = 6.5 and periods from 0.1 to 2.0 sec. The trade-off curves roughly intersect around κ = 0.02 sec and $\Delta\sigma$ = 70 bars. The curve for the shorter-period oscillators (T = 0.1 and T = 0.15 sec) are crucial for

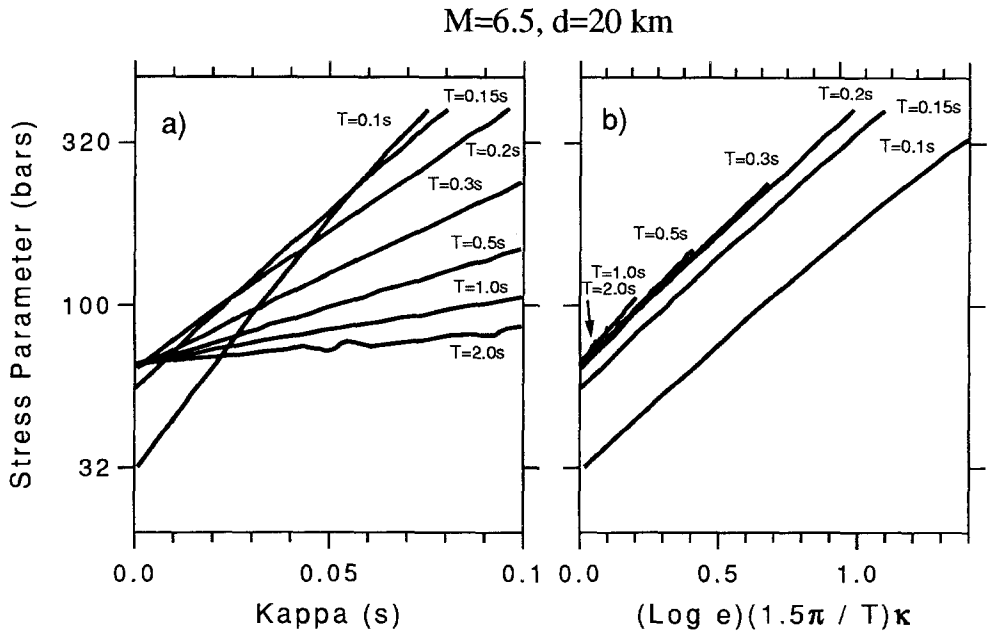

FIG. 2. (a) Superposed trade-off curves for **M** = 6.5 and r_0 = 20 km. The range of stress parameters corresponds to corner periods from somewhat less than 4 sec (300 bars) to more than 8 sec (30 bars). (b) The trade-off curves in Figure 2a, plotted against a scaled abscissa (as suggested by equation 2).

determining κ, and the curves for the longer-period oscillators define $\Delta\sigma$. Including even shorter-period response spectra would improve resolution on κ, but, because of problems with instrument corrections of the older strong-motion data (e.g., Joyner and Boore, 1988) and the possible contamination of the motions by soil-foundation interactions in recordings from single and two story structures, we do not trust the empirical values of response spectra at shorter periods. Analysis of data acquired in the last 10 years, along with reprocessing of earlier data, should provide more reliable estimates of the short-period response spectra.

To further illustrate the relevance of equation (2), we plot in Figure 2b the trade-off lines in Figure 2a against $(3\pi/2T)\kappa$. Equation (2) indicates that the slopes of these graphs should all be equal to 1 with intercepts $\log(D(T)/\sqrt{M_0})$. The slopes of the curves are close to, but not equal to, 1. There also is a slight systematic decrease in slope with decreasing period. These deviations reflect the approximate nature of the factor of $3\pi/2T$ in the exponent of equation (2).

One problem with a plot of trade-off curves alone is that they do not convey how much or little relief surrounds each curve: the curves simply follow the bottom of the valley formed by the absolute value of the residuals. To get a better sense for the uncertainty in choosing $\Delta\sigma$ and κ, the maximum absolute residual over the range of oscillator periods from 0.1 to 2.0 sec was computed for each pair of the parameters; the results are shown in Figure 3 for magnitudes 5.5, 6.5, and 7.5 (the previous figures were for magnitude 6.5 only). The residual patterns and the smallest residuals (close to 0.1 log units) are similar for the three magnitudes.

To better demonstrate the ability of the stochastic model to fit the empirical data for a range of earthquake sizes, we show in Figure 4 the maximum absolute residual over all three magnitudes. This is the most demanding measure of how well the stochastic model fits the observations; a pair of $\Delta\sigma$ and κ chosen within the 0.15 contour would result in ground motion predictions that were within a factor of 1.4 of the actual motions for all periods from 0.1 to 2.0 sec and magnitudes from 5.5 to 7.5. Two contour plots are shown; the *left* plot shows the maximum residuals over the period range of 0.1 to 2.0 sec, and the *right* plot shows the maximum residuals when the lowest period oscillator (0.1 sec) is excluded. We show the latter figure because the smallest maximum residual in Figure 4a occurs for $T = 0.1$ sec, and we have some misgivings about how well the empirical value is determined at this period, for reasons given earlier. The best choice of κ and $\Delta\sigma$ does not strongly depend on which plot is used, although for Figure 4b the smallest maximum residual (0.08) occurs for a single value of κ and $\Delta\sigma$ (0.015 sec and 71 bars, respectively), whereas in Figure 4a two pairs of κ and $\Delta\sigma$ values ((0.02 sec, 71 bars) and (0.03 sec, 100 bars)) give almost equally small residuals (0.13 units).

The contour plots are useful in that they show the maximum difference between the empirical results and the stochastic model over a range of magnitudes and periods for any value of κ and $\Delta\sigma$; they do not show, however, mismatches that might be a systematic function of magnitude or period. In Figure 5, we show the pseudo-velocity response spectra corresponding to the κ and $\Delta\sigma$ values that give the smallest values for the maximum residuals in Figures 4a and b. Even though the maximum residual in Figures 5a and b is almost the same, the systematic mismatch at the longer periods shown in Figure 5b argues against a stress parameter of 100 bars.

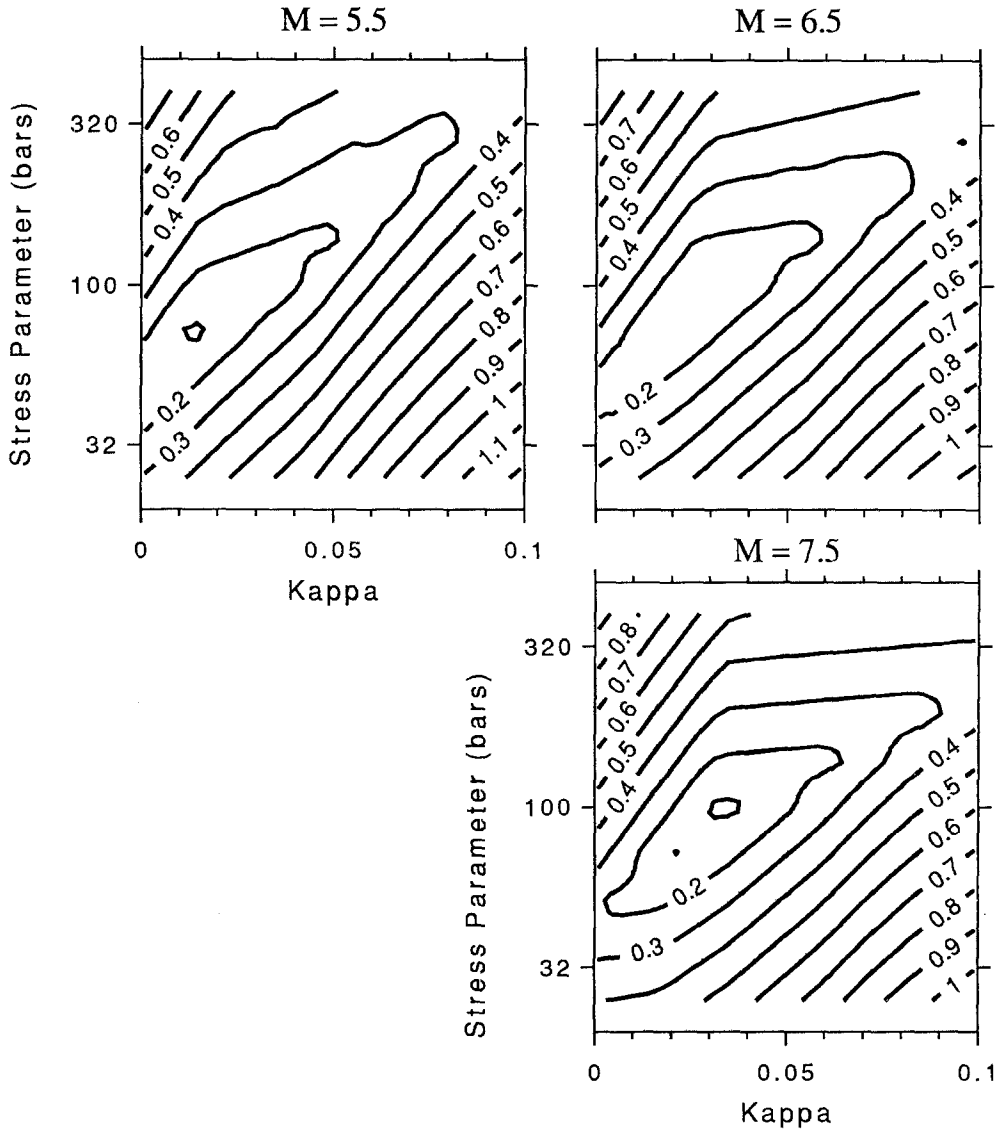

FIG. 3. Contours of maximum absolute residual for individual magnitudes over the range of oscillator periods from 0.1 to 2.0 sec. For purposes of contouring the results, the motions were interpolated to a finer grid using bilinear interpolation (e.g., Press *et al.*, 1986, p. 96).

The best match between observations and the stochastic model is given for κ and $\Delta\sigma$ close to 0.02 sec and 70 bars, respectively. The smallest maximum absolute residual for the grid used in this note is attained for $\kappa = 0.015$ sec and $\Delta\sigma = 71$ bars if the residuals at $T = 0.1$ sec are excluded and for $\kappa = 0.02$ sec and $\Delta\sigma = 71$ bars otherwise. The maximum residuals in both cases correspond to factors of 1.2 and 1.3, small errors considering the simplicity of the model and the range of magnitudes and oscillator periods.

DISCUSSION

The best values of $\Delta\sigma$ near 70 bars and κ close to 0.02 sec are similar to those used by Boore (1986). In his Figure 9, he showed that peak velocity and

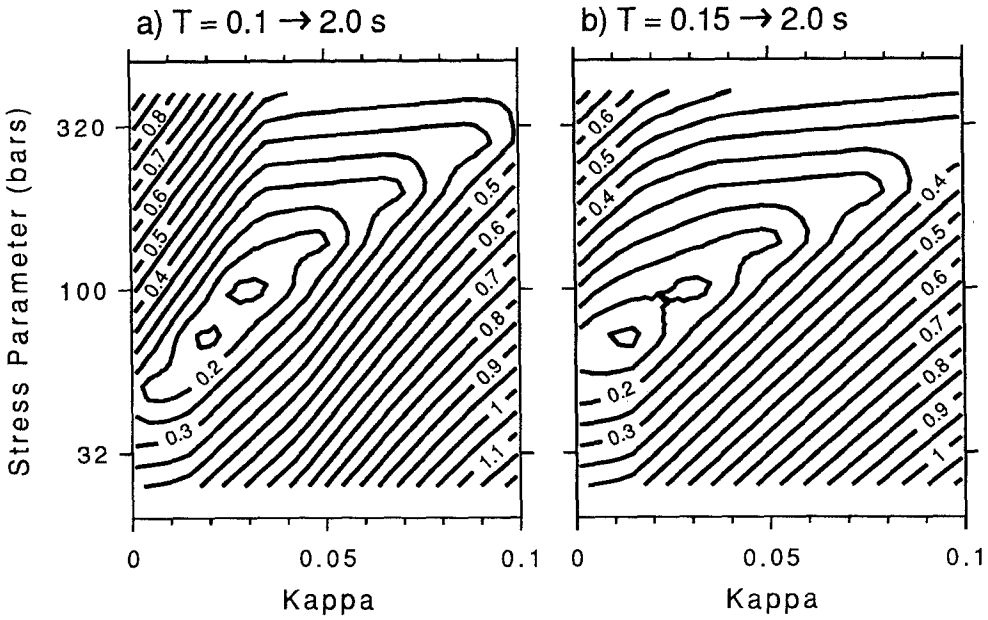

FIG. 4. Contour of maximum absolute residual for magnitudes 5.5, 6.5, and 7.5 combined (in other words, the result of picking the maximum residual from the three contour plots of Fig. 3 for each pair of $\Delta\sigma$ and κ). To better define the region of minimum residual, a contour interval of 0.05 log units was used rather than 0.1 as in the previous figures. Part (a) contains the residuals for the period range 0.1 to 2.0 sec, while the residuals shown in part (b) were obtained by excluding the residuals for the 0.1-sec oscillator.

peak acceleration can be fit approximately with $\Delta\sigma = 50$ bars and a high-frequency diminution parameter between $\kappa = 0.04$ sec and $f_{max} = 15$ Hz (this f_{max} is equivalent to $\kappa = 0.01$ sec if rms acceleration is preserved).

Although the parameters found in this note provide the best match of the stochastic model to the observed ground motions, they should be used with caution. The Joyner and Boore (1988) representation of reality is based on data only up to 1980. Many more data are now available, and new empirical equations are being developed. Furthermore, we note that our "κ" may be different than that determined using the spectral fitting procedure of Anderson and Hough (1984): in their procedure κ is strongly influenced by the behavior of the Fourier spectra at frequencies above the apparent f_{max} (usually above 5 Hz), whereas the response spectral results depend little on this frequency range. It might turn out that, although the κ derived from this study is fine for predicting response spectra to periods as short as 0.15 to 0.1 sec, it does not correspond to the κ that would be measured using the semilog method of Anderson and Hough.

Even though the particular values of $\Delta\sigma$ and κ may change with more data, the methodology we have applied should be useful in deriving parameters of the stochastic model from observed ground motions.

ACKNOWLEDGMENTS

Conversations with Don Bernreuter and Walter Silva motivated the study reported here. We thank Tom Hanks and Walt Silva for reviewing the paper. The research reported here was supported by the Nuclear Regulatory Commission.

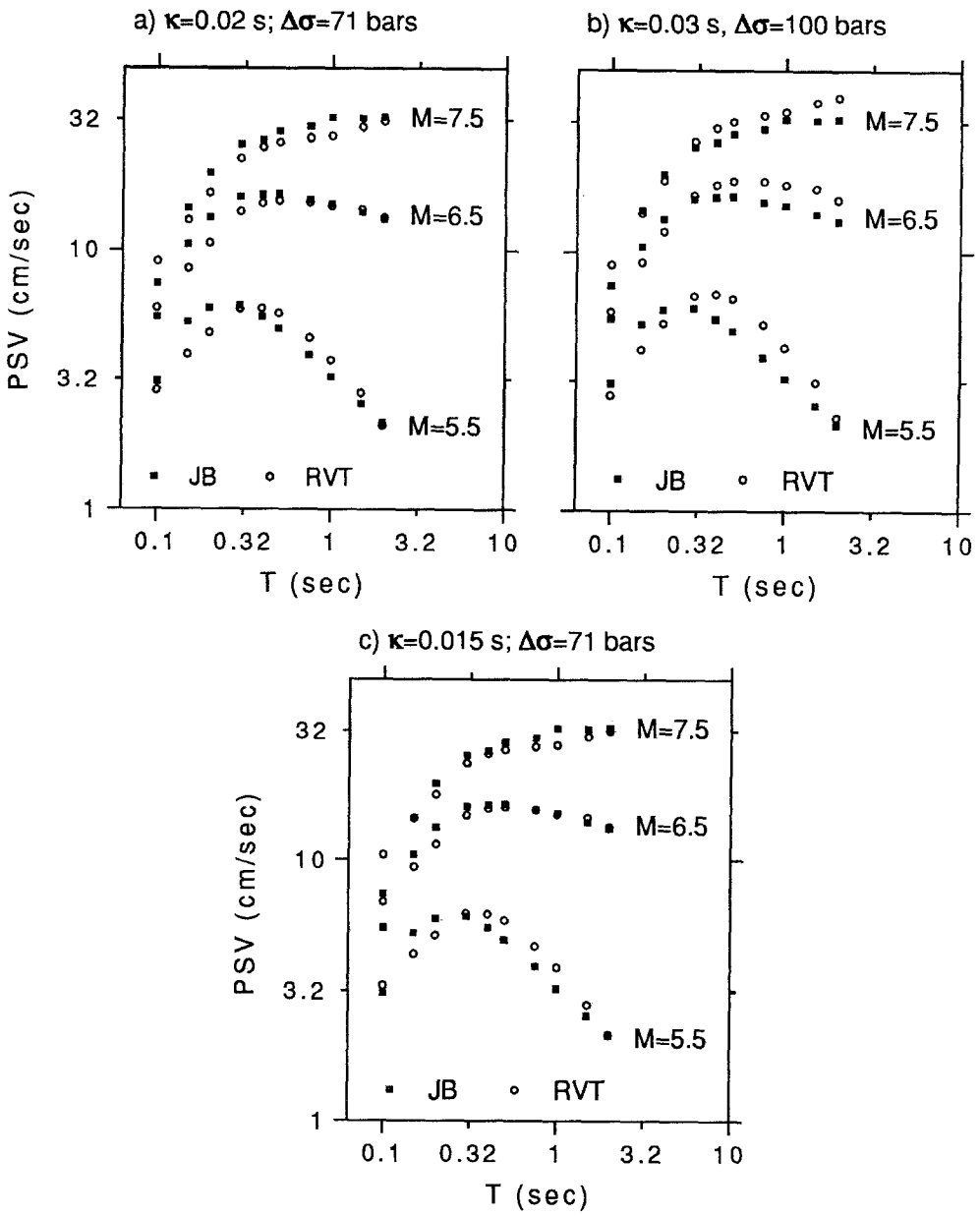

FIG. 5. Comparison of pseudo-velocity response spectra (*PSV*) from the empirical analysis of Joyner and Boore (*JB*) and the stochastic model (*RVT*). Parts (a) and (b) of the figure correspond to the κ and $\Delta\sigma$ values given by the two minima within the 0.15 contour in Figure 4a, and the parameter values used for the stochastic model in part (c) give the smallest maximum residual in Figure 4b.

REFERENCES

Anderson J. G. and S. E. Hough (1984). A model for the shape of the Fourier amplitude spectrum of acceleration at high frequencies, *Bull. Seism. Soc. Am.* **74**, 1969–1993.

Atkinson, G. M. (1984). Attenuation of strong ground motion in Canada from a random vibrations approach, *Bull. Seism. Soc. Am.* **74**, 2629–2653.

Boore, D. M. (1983). Stochastic simulation of high-frequency ground motions based on seismological models of the radiated spectra, *Bull. Seism. Soc. Am.* **73**, 1865–1894.

Boore, D. M. (1986). Short-period *P*- and *S*-wave radiation from large earthquakes: implications for spectral scaling relations, *Bull. Seism. Soc. Am.* **76**, 43–64.

Boore, D. M. and G. M. Atkinson (1987). Stochastic prediction of ground motion and spectral response parameters at hard-rock sites in eastern North America, *Bull. Seism. Soc. Am.* **77**, 440–467.

Boore, D. M. and W. B. Joyner (1991). Estimation of ground motion at deep soil sites in eastern North America, *Bull. Seism. Soc. Am.* **81**, 2167–2185.

Chin, B.-Y. and K. Aki (1991). Simultaneous study of the source, path, and site effects on strong ground motion during the 1989 Loma Prieta earthquake: a preliminary result on pervasive nonlinear site effects, *Bull. Seism. Soc. Am.* **81**, 1859–1884.

Hanks, T. C. (1982). f_{max}, *Bull. Seism. Soc. Am.* **72**, 1867–1879.

Hanks, T. C. and D. M. Boore (1984). Moment-magnitude relations in theory and practice, *J. Geophys. Res.* **89**, 6229–6235.

Hanks, T. C. and R. K. McGuire (1981). The character of high-frequency strong ground motion, *Bull. Seism. Soc. Am.* **71**, 2071–2095.

Joyner, W. B. (1984). A scaling law for the spectra of large earthquakes, *Bull. Seism. Soc. Am.* **74**, 1167–1188.

Joyner, W. B. and D. M. Boore (1988). Measurement, characterization, and prediction of strong ground motion, in *Proc. of Earthquake Eng. Soil Dyn. II*, GT Div/ASCE, Park City, Utah, 27—30 June 1988, 43–102.

Ou, G.-B. and R. B. Herrmann (1990). A statistical model for ground motion produced by earthquakes at local and regional distances, *Bull. Seism. Soc. Am.* **80**, 1397–1417.

Press, W. H., B. P. Flannery, S. A. Teukolsky, and W. T. Vetterling (1986). *Numerical Recipes: The Art of Scientific Computing*, Cambridge University Press, Cambridge, England.

Rovelli, A., M. Cocco, R. Console, B. Alessandrini, and S. Mazza (1991). Ground motion waveforms and source spectral scaling from close-distance accelerograms in a compressional regime area (Friuli, northwestern Italy), *Bull. Seism. Soc. Am.* **81**, 57–80.

Silva, W., R. Darragh, C. Stark, I. Wong, J. Stepp, J. Schneider, and S. Chiou (1990). A methodology to estimate design response spectra in the near-source region of large earthquakes using the band-limited-white-noise ground motion model, in *Proc. of the 4th U.S. Conf. on Earthquake Eng.* **1**, 487–494.

Stepp, C., W. Silva, H. B. Seed, I. M. Idriss, R. McGuire, and J. Schneider (1991). Site response evaluations based upon generic soil profiles using random vibration methodology, in *Proc. 4th Int. Conf. on Seismic Zonation* **III**, 739–746.

Toro, G. R. and R. K. McGuire (1987). An investigation into earthquake ground motion characteristics in eastern North America, *Bull. Seism. Soc. Am.* **77**, 468–489.

U. S. GEOLOGICAL SURVEY
MAIL STOP 977
345 MIDDLEFIELD ROAD
MENLO PARK, CALIFORNIA 94025

Manuscript received 8 October 1991